Fundamental diagrams for multidirectional pedestrian flows

J. Stat. Mech. (2017) 033404

(http://iopscience.iop.org/1742-5468/2017/3/033404)

Journal of Statistical Mechanics: Theory and Experiment
An IOP and SISSA journal

PAPER: Interdisciplinary statistical mechanics

Fundamental diagrams for multidirectional pedestrian flows

Shuchao Cao[1,2], Armin Seyfried[2], Jun Zhang[2], Stefan Holl[2] and Weiguo Song[1,3]

[1] State Key Laboratory of Fire Science, University of Science and Technology of China, Hefei 230027, People's Republic of China
[2] Forschungszentrum Jülich GmbH, Institute for Advanced Simulation, 52425 Jülich, Germany
E-mail: wgsong@ustc.edu.cn

Received 26 September 2016, revised 30 January 2017
Accepted for publication 21 February 2017
Published 23 March 2017

Online at stacks.iop.org/JSTAT/2017/033404
https://doi.org/10.1088/1742-5468/aa620d

Abstract. Fundamental diagrams for uni-, bi- and multidirectional flows at corridors and crossings are investigated by a series of experiments under laboratory conditions. At high densities pedestrians are forced to make detours or even change the intended destinations. These unintended movements lead to an overestimation of the performance of crossings. To consider these effects in the determination of the capacities the fundamental diagrams are measured using advanced methods. In comparison to classical methods, significant differences relating to the capacities are found. The fundamental diagrams are compared with data of uni-, bi-, and multidirectional flows and with data of the literature.

Keywords: traffic and crowd dynamics

[3] Author to whom any correspondence should be addressed.

1742-5468/17/033404+18$33.00

Contents

1. Introduction **2**

2. Experiment setup **3**

3. Measurement methods **7**
3.1. Methods A1, A2 and A3 7
3.2. Method D1 and D2 9

4. Results and analysis **12**
4.1. Comparison of measurement methods 13
4.2. Comparison of different pedestrian flows 15

5. Conclusion **17**

Acknowledgments **17**

References **17**

1. Introduction

Compared to vehicle traffic pedestrian traffic is more complex. Vehicle traffic is largely regulated by lanes, traffic lights or rules, while pedestrian traffic is mostly unregulated. Therefore, a description of the pedestrian system by transport characteristics is challenging and classical methods for measuring the performance of the traffic system have to be scrutinized regarding their usability in more complex situations. In this article we study unregulated multidirectional pedestrian streams at crossings as one of the most usual but also most complex traffic system.

Up to now, many pedestrian experiments, including unidirectional flow [1], bidirectional counter flows [2–6] and bottleneck flow [7–11], have been conducted. For bidirectional cross flows some experiments [12–15] were also carried out. In [3] it was shown that the maximum specific flow of the unidirectional stream was significantly higher than of bidirectional counter flows. For fundamental diagrams of bidirectional counter flows and bidirectional cross flows, contradictory results could be found in the literature. Wong *et al* [12] found a decreasing capacity when the cross angle increased. The lowest capacity was found in counter streams. Contrarily Zhang *et al* [14] found no difference for selected density intervals in the congested branch of the fundamental diagrams between bidirectional cross flows with a cross angle of 90° and bidirectional counter flows. This comparison indicates that the characteristic of perpendicular cross flows still needs more investigation.

In bidirectional streams pedestrians only consider conflicts with pedestrians from the same or the other direction, while in multidirectional streams pedestrians have to anticipate conflicts with people from multiple directions. Current studies on multidirectional flows are still few. To our best knowledge, only Lian *et al* [16] conducted experiments with four-directional cross pedestrian flows. The global and local density-velocity

J. Stat. Mech. (2017) 033404

relations in the cross area were compared. It was found that the specific flow increased for the density $\rho < 5$ m^{-2} and the maximum specific flow reached 1.8 (m $\cdot$ s)$^{-1}$, which was close to the specific flow of unidirectional stream and much higher than of bidirectional counter flows [3] around $\rho = 5$ m^{-2}. The exceptional specific flow and density has to be scrutinized and more experimental data are needed to investigate the pedestrian dynamics of multidirectional flows, especially the fundamental diagrams.

In previous studies of pedestrian flow, different measurement methods were used. Large discrepancies between different measurement methods could already be found in single-file experiment [17]. For the analysis of unidirectional flow, Zhang *et al* [1] introduced four measurement methods to calculate pedestrian flow, density and velocity. No significant differences are found in the fundamental diagrams except for different fluctuations and an improved resolution of the shape. Multidirectional flows at crossings are even more complex. Therefore, it is necessary to extend and revise the analysis based on classical measurement methods to consider directional splits of turning, forced detours and changes in the intended destination due to congestion.

Based on the problems mentioned above, uni-, bi- and multidirectional flows are analyzed in the following. The paper is organized as follows. In section 2, we give a detailed introduction of the pedestrian experiments. Different measurement methods are proposed in section 3. In section 4, the characteristics of different pedestrian flows under different conditions are investigated and compared with previous studies. In section 5, the conclusions are made and the paper is closed.

2. Experiment setup

To study different pedestrian flows, experiments under laboratory conditions were carried out. About 2000 people participated in the BaSiGo experiments performed in Düsseldorf in 2013. Most of them were university students with a mean age of 25 years. In this paper, the unidirectional flow (BaSiGo_UO), bidirectional counter flow (BaSiGo_BO), bidirectional cross flow (BaSiGo_Cross_D) and four-directional cross flow (BaSiGo_Cross_A) experiments were analyzed. Before each run of experiment, the test people were instructed to move along a specific direction called 'intended direction'. For crossing experiments the intended direction was straight without directional split. In figure 1 arrows indicate the intended directions and different colors are used to allow a differentiation in case of multiple intended directions. The length of the corridor is 12 m and 10 m in figures 1(a) and (b) respectively. In the cross experiments as shown in figures 1(c) and (d), pedestrians moved to their opposite directions, which means if pedestrians' initial positions were in the left (right, top and bottom) of the cross area, they went to the right (left, bottom and top), namely moved along the $x+$ ($x-$, $y-$ and $y+$) direction. The length of the corridor in each side is 5 m. The areas marked by dashed lines in figure 1 indicate the measurement areas with the following sizes: (a) BaSiGo_UO ($a = 4$ m, $b_{\mathrm{cor}} = 5$ m), (b) BaSiGo_BO ($a = b_{\mathrm{cor}} = 4$ m), (c) BaSiGo_Cross_D ($b_{\mathrm{cor}} = 4$ m), (d) BaSiGo_Cross_A ($b_{\mathrm{cor}} = 4$ m). To realize a variation of density values for every experiment different runs were performed. For the experiment of unidirectional stream the width of the entrance b_{in} and exit b_{out} was

J. Stat. Mech. (2017) 033404

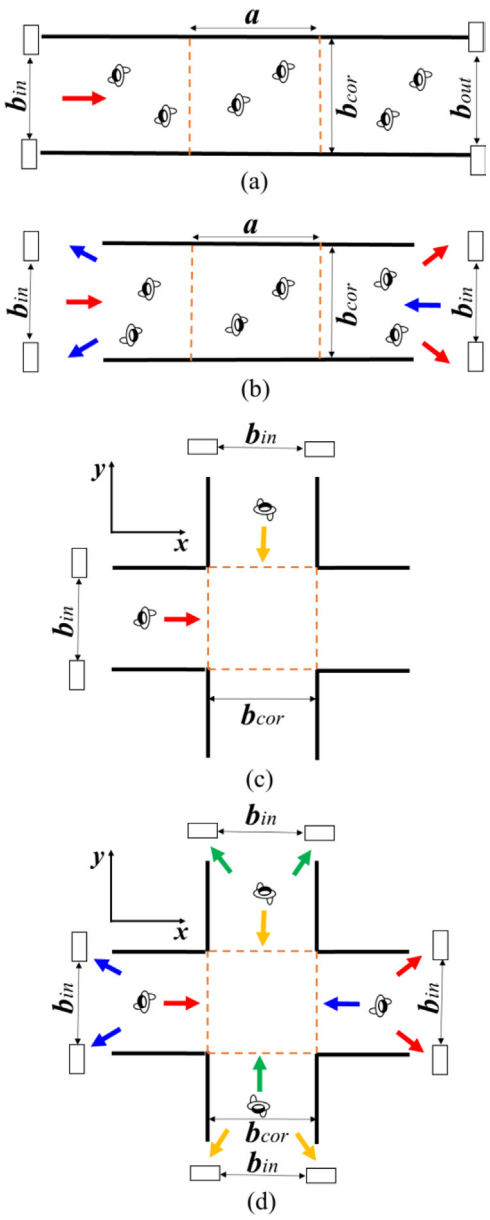

Figure 1. Sketches of the BaSiGo experiments. The arrows with different colors indicate pedestrian's intended directions and the dashed lines mark the measurement areas. (a) BaSiGo_UO, (b) BaSiGo_BO, (c) BaSiGo_Cross_D, (d) BaSiGo_Cross_A.

varied for each run. For experiments with bi- and multidirectional streams the width of the different entrances b_{in} was changed. The details of all runs of the experiments are shown in tables 1–4 respectively.

We used a camera grid of six by four cameras (with a resolution of 1280 × 1024), mounted 7.5 m above the floor, which covered a little over 10 m by 10 m at ground level; further technical details of cameras can be found in [20, 21]. All the experiments were recorded by cameras. Finally, the pedestrian trajectories were automatically extracted

Table 1. The BaSiGo_UO (unidirectional flow) experiment.

Run	Name	b_{in} (m)	b_{cor} (m)	b_{out} (m)	N
01	uni_corr_500_01	1.0	5.0	5.0	148
02	uni_corr_500_02	2.0	5.0	5.0	760
03	uni_corr_500_03	3.0	5.0	5.0	916
04	uni_corr_500_04	4.0	5.0	5.0	909
05	uni_corr_500_05	5.0	5.0	5.0	905
06	uni_corr_500_06	5.0	5.0	4.0	913
07	uni_corr_500_07	5.0	5.0	3.0	914
08	uni_corr_500_08	5.0	5.0	2.0	477
09	uni_corr_500_09	5.0	5.0	1.0	310
10	uni_corr_500_10	5.0	5.0	0.6	273

Table 2. The BaSiGo_BO (bidirectional counter flows) experiment.

Run	Name	b_{in} (m)	b_{cor} (m)	N
01	bi_corr_400_b_01	0.6	4.0	141
02	bi_corr_400_b_02	0.9	4.0	259
03	bi_corr_400_b_03	1.2	4.0	480
04	bi_corr_400_b_04	1.8	4.0	743
05	bi_corr_400_b_05	2.4	4.0	643
06	bi_corr_400_b_06	3.0	4.0	830
07	bi_corr_400_b_07	4.0	4.0	606
08	bi_corr_400_b_08	4.0	4.0	703
09	bi_corr_400_b_09	2.4	4.0	483
10	bi_corr_400_b_10	4.0	4.0	736

Table 3. The BaSiGo_Cross_D (bidirectional cross flows) experiment.

Run	Name	b_{in} (m)	b_{cor} (m)	N
01	CROSS_90_D_1	0.6	4.0	603
02	CROSS_90_D_2	0.9	4.0	604
03	CROSS_90_D_3	1.2	4.0	606
05	CROSS_90_D_5	1.8	4.0	600
06	CROSS_90_D_6	2.4	4.0	597
07	CROSS_90_D_7	3.0	4.0	604
08	CROSS_90_D_8	4.0	4.0	592

Table 4. The BaSiGo_Cross_A (four-directional cross flows) experiment.

Run	Name	b_{in} (m)	b_{cor} (m)	N
01	CROSS_90_A_01	0.6	4.0	247
02	CROSS_90_A_02	0.6	4.0	439
03	CROSS_90_A_03	0.9	4.0	323
04	CROSS_90_A_04	1.2	4.0	352
05	CROSS_90_A_05	1.5	4.0	337
06	CROSS_90_A_06	2.0	4.0	269
07	CROSS_90_A_07	0.6	4.0	323
08	CROSS_90_A_08	1.5	4.0	298
09	CROSS_90_A_09	4.0	4.0	299
10	CROSS_90_A_10	4.0	4.0	324

J. Stat. Mech. (2017) 033404

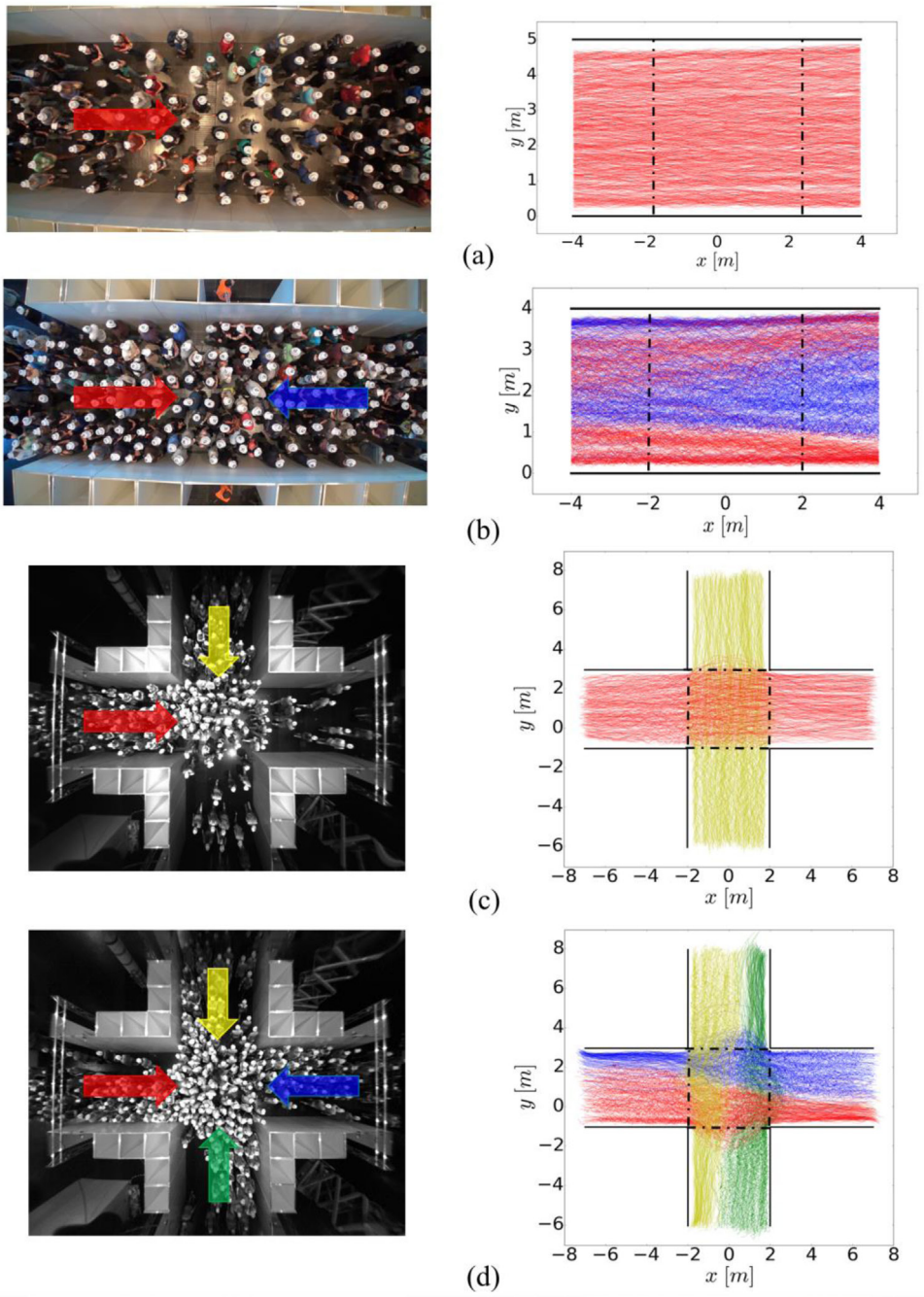

Figure 2. Snapshots and cumulative trajectories of selected runs of the BaSiGo experiments. Arrows in the left figure indicate pedestrian's intended directions and the dashed lines in the right figure are reference lines which mark the measurement areas. (a) BaSiGo_UO, (b) BaSiGo_BO, (c) BaSiG_Cross_D, (d) BaSiGo_Cross_A.

from video recordings using the software *PeTrack* [18, 19] and a marker-based tracking algorithm [20, 21]. Figure 2 shows the experiment snapshots and the corresponding trajectories. Pedestrian characteristics including the flow, density and velocity are calculated from these trajectories in the following.

J. Stat. Mech. (2017) 033404

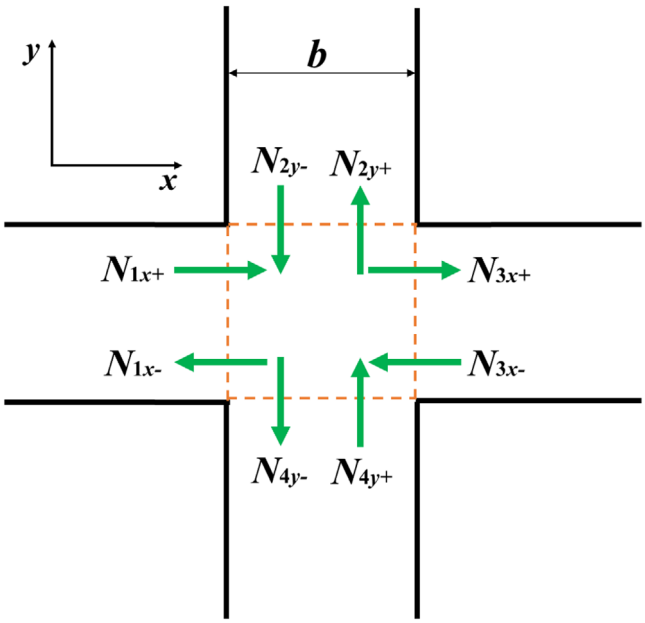

Figure 3. Scenario of the four-directional cross flows experiment (BaSiGo_Cross_A). The dashed lines (left line 1, upper line 2, right line 3, and lower line 4) denote the reference lines which mark the measurement area, and the arrows indicate the movement direction of pedestrians.

3. Measurement methods

In this section, we extend and revise the classical measurement method A and method D proposed in [1] for uni-, bi- and multidirectional flows at corridors and crossings. The measurement areas in different experiment scenarios have been defined and marked as shown in figures 1 and 2. In order to distinguish with other measurement methods, the extensions of original method A and method D [1] are called method A1 and method D1 respectively in our paper. We take the four-directional cross flows as an example to introduce them in the following.

3.1. Methods A1, A2 and A3

In method A1 reference lines are defined along the border of the measurement area and the mean values of flow and density are calculated over a period of time Δt.

In figure 3, the specific flow J_s and density ρ are calculated as follows:

$$\rho = \frac{N_A}{A}, \; A = b \cdot b \tag{1}$$

where b is the width of measurement area; the density ρ is the number of pedestrians N_A in the measurement area divided by the measurement area size A. N_A is determined independently from the flow measurement methods introduced in the next;

$$N_{in} = N_{1x+} + N_{2y-} + N_{3x-} + N_{4y+} \tag{2}$$

where N_{1x+} means the number of pedestrians moving along $x+$ direction and across the reference line 1. Similarly, N_{1x-}, N_{2y+}, N_{2y-}, N_{3x+}, N_{3x-}, N_{4y+} and N_{4y-} represent the

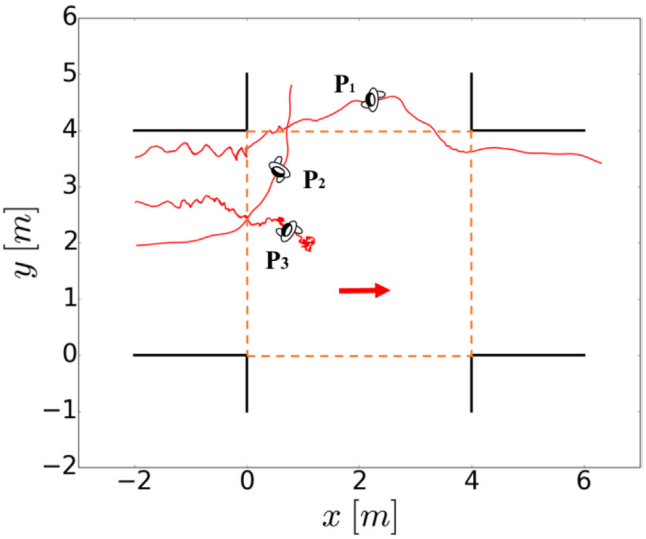

Figure 4. Exemplary trajectories observed in the experiments. The red solid lines denote pedestrians' real trajectories. The dashed lines are the reference lines. The arrow indicates pedestrians' intended direction. Pedestrian P_1 makes a detour; pedestrian P_2 changes the intended destination; pedestrian P_3 sways the body frequently and moves back and forth in the cross area.

pedestrian number with the corresponding movement direction and across the corresponding reference line; N_{in} is the total pedestrian number crossing the reference line and entering the measurement area;

$$N_{\text{out}} = N_{1x-} + N_{2y+} + N_{3x+} + N_{4y-} \tag{3}$$

where N_{out} is the total pedestrian number crossing the reference line and exiting the measurement area;

$$J_{\text{in}} = \frac{\Delta N_{\text{in}}}{\Delta t}, \quad J_{\text{out}} = \frac{\Delta N_{\text{out}}}{\Delta t} \tag{4}$$

where J_{in} (J_{out}) gives the total inflow (outflow) and ΔN_{in} (ΔN_{out}) denotes the number of pedestrians who come into (get out of) the measurement area during time interval Δt ($\Delta t = 4\,\text{s}$ is used in this paper);

$$J_{\text{s,in}} = \frac{J_{\text{in}}}{b}, \quad J_{\text{s,out}} = \frac{J_{\text{out}}}{b} \tag{5}$$

where $J_{\text{s,in}}$ ($J_{\text{s,out}}$) is the specific inflow (specific outflow) and the total specific flow J_{s} is given as:

$$J_{\text{s}} = \frac{J_{\text{s,in}} + J_{\text{s,out}}}{2}. \tag{6}$$

According to method A1 extended based on [1] each pedestrian is counted only once at each measurement line, to avoid counting of oscillations due to head movement at the measurement lines. However, high densities trajectories which do not contribute to the outflow with respect to the intended direction could be observed as shown in figure 4. The exemplary trajectories in figure 4 show the following problems: case (1) detour. In

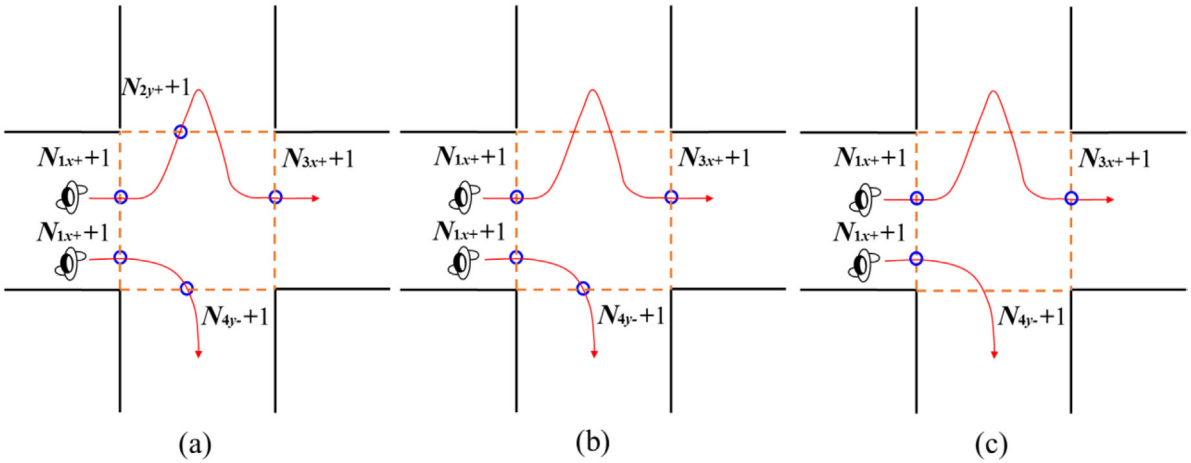

Figure 5. Pedestrian number counted with (a) method A1, (b) method A2 and (c) method A3. The dashed lines denote the reference lines. The red solid lines are pedestrians' schematic trajectories.

high densities many people move to the cross area at the same time. In order to get out of cross area quickly, pedestrian P_1 makes a detour to avoid a crowd in the cross area, which indicates he/she is also counted on the upper reference line in method A1; case (2) change of the intended destination. Pedestrian P_2 changes the intended direction and goes to another destination than original intended. Using the measurement method introduced in equations (1)–(6) this person contributes to the flow. But considering the flow in the intended direction this movement does not contribute because he/she does not achieve the intended goal successfully.

The cases mentioned above are not taken into account by method A1, which means that the counted number of pedestrians crossing the reference lines cannot reflect the effective flow through the cross area. Revisions are made to solve these problems in the following:

Method A2 based on method A1 considers case (1). In this method a pedestrian is counted only two times: (1) the first time he/she crosses the reference line and enters into the measurement area; (2) the last time he/she crosses the reference and gets out of the cross area. Therefore, we can see one pedestrian cross the upper reference line but she/he is not counted in N_{2y+} and N_{2y-} in figure 5(b).

Method A3 based on method A2 takes into account pedestrian's intended direction to solve case (2). In figure 5(c) one pedestrian crosses the lower reference line and finally goes to the original unintended destination. Therefore, the pedestrian is only counted the first time she/he enters into the measurement area.

Essentially, the difference among methods A1, A2 and A3 is the way of calculating the number of pedestrians crossing the reference lines as displayed in figure 5.

3.2. Method D1 and D2

Method D1 is based on the Voronoi diagram, which has been used in many fields [22–26]. At any time the positions of pedestrians are represented as a set of points from which the Voronoi diagrams are generated.

In method D1, the specific flow J_s, density ρ and velocity v are calculated as follows:

$$\rho_{xy} = \begin{cases} 1/A_i(t) & \text{if}(x, y) \in A_i(t) \\ 0 & \text{else} \end{cases} \tag{7}$$

where ρ_{xy} is the density distribution of the space; $A_i(t)$ gives the Voronoi cell area for person i;

$$v_{xy} = \begin{cases} \sqrt{v_{ix}(t)^2 + v_{iy}(t)^2} & \text{if}(x, y) \in A_i(t) \\ 0 & \text{else} \end{cases} \tag{8}$$

where v_{xy} is the velocity distribution of the space; $v_{ix}(t)$ and $v_{iy}(t)$ denote the vectors of velocity in x axis and y axis respectively;

$$v_{ix}(t) = \frac{x_i(t + \Delta t'/2) - x_i(t - \Delta t'/2)}{\Delta t'},\ v_{iy}(t) = \frac{y_i(t + \Delta t'/2) - y_i(t - \Delta t'/2)}{\Delta t'} \tag{9}$$

where $\Delta t'$ is the time interval to calculate velocity and $\Delta t' = 0.4\,\text{s}$ is adopted in this paper;

$$\rho = \frac{\iint \rho_{xy} \mathrm{d}x\mathrm{d}y}{A}, \quad v = \frac{\iint v_{xy} \mathrm{d}x\mathrm{d}y}{A} \tag{10}$$

$$J_s = \rho \cdot v. \tag{11}$$

Nevertheless, the same problems just as discussed in section 3.1 also exist in method D1. The effects of detour (P_1 in figure 4), changing the intended destination (P_2 in figure 4), body sway and moving back (P_3 in figure 4) on the calculation of flow are not removed in method D1. Therefore, we revise method D1 and propose method D2 in the following:

In method D2 two changes are made based on method D1: (1) we calculate the flow considering the pedestrian's intended direction, which means pedestrians only contribute to the flow in the intended direction and the effect of body sway is eliminated; (2) if one pedestrian moves back, his/her contribution to the total flow is zero. Therefore the contribution of moving back to the flow is removed. The calculations of density and flow are the same with method D1 (equations (7)–(11)). The calculation of velocity in equation (8) in method D1 is revised in method D2 as follows:

$$v_{xy} = \begin{cases} v_{ix+}(t) = \begin{cases} v_{ix}(t) & \text{if } \text{ped}_{\text{dir}} \text{ is } x+ \text{ and } v_{ix}(t) > 0 \\ 0 & \text{else} \end{cases} \\ v_{ix-}(t) = \begin{cases} v_{ix}(t) & \text{if } \text{ped}_{\text{dir}} \text{ is } x- \text{ and } v_{ix}(t) < 0 \\ 0 & \text{else} \end{cases} \\ v_{iy+}(t) = \begin{cases} v_{iy}(t) & \text{if } \text{ped}_{\text{dir}} \text{ is } y+ \text{ and } v_{iy}(t) > 0 \\ 0 & \text{else} \end{cases} \\ v_{iy-}(t) = \begin{cases} v_{iy}(t) & \text{if } \text{ped}_{\text{dir}} \text{ is } y- \text{ and } v_{iy}(t) < 0 \\ 0 & \text{else} \end{cases} \\ 0 \end{cases} \quad \begin{array}{l} \text{if}(x, y) \in A_i(t) \\ \\ \\ \\ \\ \text{else} \end{array} \tag{12}$$

J. Stat. Mech. (2017) 033404

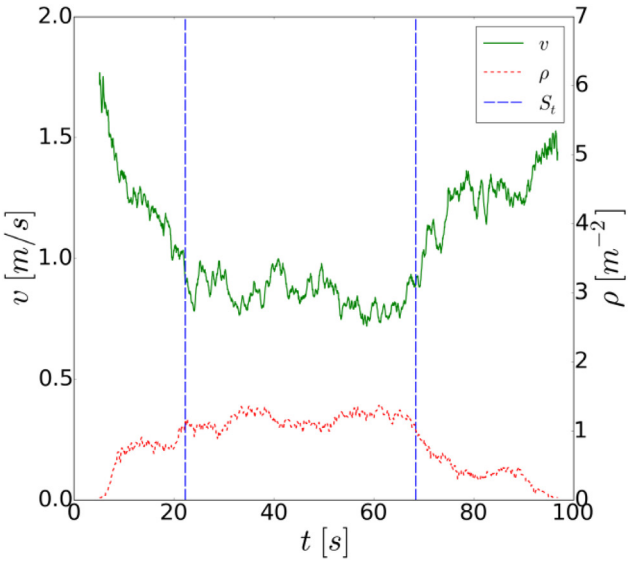

Figure 6. Time series and steady state for a run of CROSS_90_A_10. The red dashed and green solid lines represent the density and velocity respectively. The blue vertical lines mark the steady state.

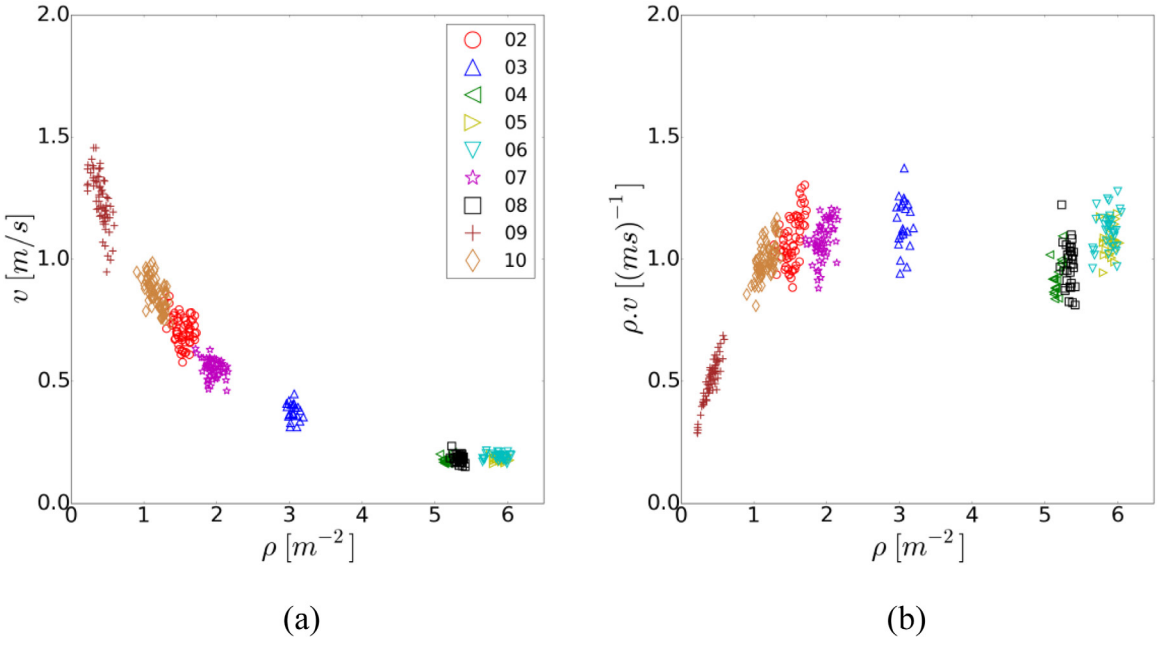

Figure 7. Fundamental diagrams of BaSiGo_Cross_A experiment measured with method D1. Data of the steady state from different runs are marked with different symbols and colors. (a) Density-velocity relation, (b) density-flow relation.

where ped_{dir} indicates the pedestrian's intended direction; $v_{ix+}(t)$, $v_{ix-}(t)$, $v_{iy+}(t)$ and $v_{iy-}(t)$ denote the components of the pedestrian's velocity in the $x+$, $x-$, $y+$ and $y-$ directions respectively. In essence, methods D1 and D2 are different on the consideration of the contribution of velocity to the pedestrian flow.

https://doi.org/10.1088/1742-5468/aa620d

J. Stat. Mech. (2017) 033404

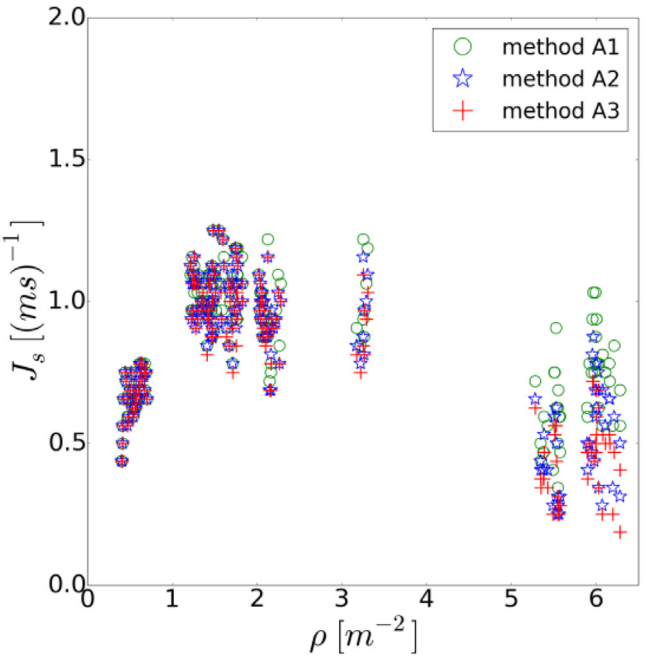

Figure 8. Comparison of fundamental diagrams of BaSiGo_Cross_A experiment with methods A1, A2 and A3.

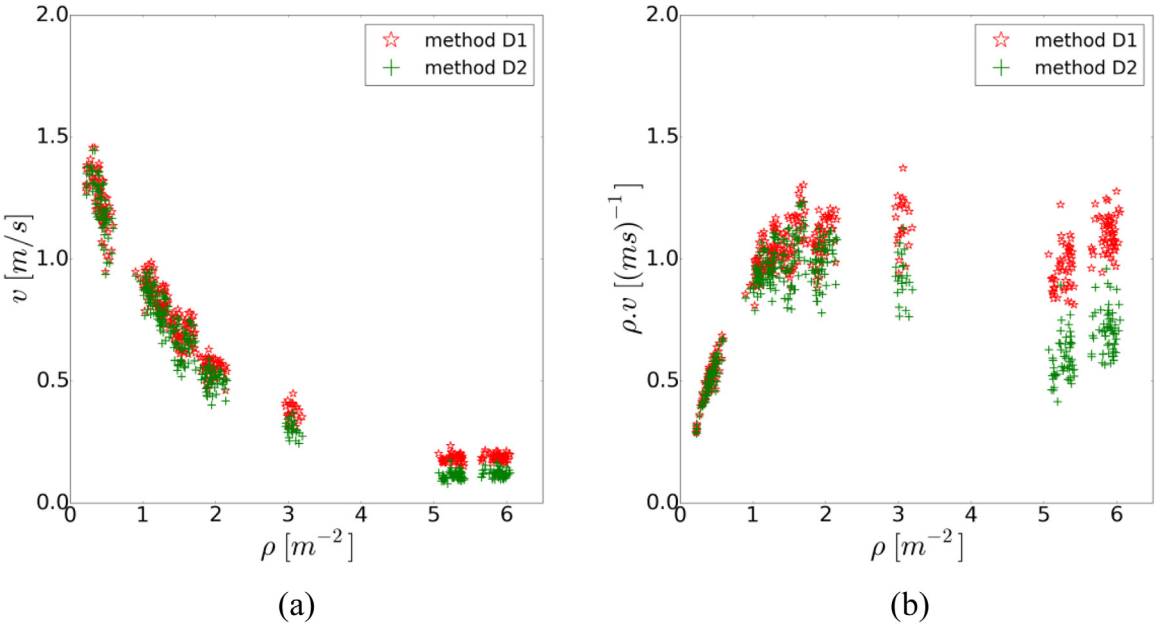

Figure 9. Comparison of fundamental diagrams of BaSiGo_Cross_A experiment with methods D1 and D2. (a) Density–velocity relation, (b) density–flow relation.

4. Results and analysis

For the determination of the fundamental diagrams only data from the steady state are used. Figure 6 shows the time series of the velocity and the density for one run of BaSiGo_Cross_A experiment. To identify the steady state the method described in [8]

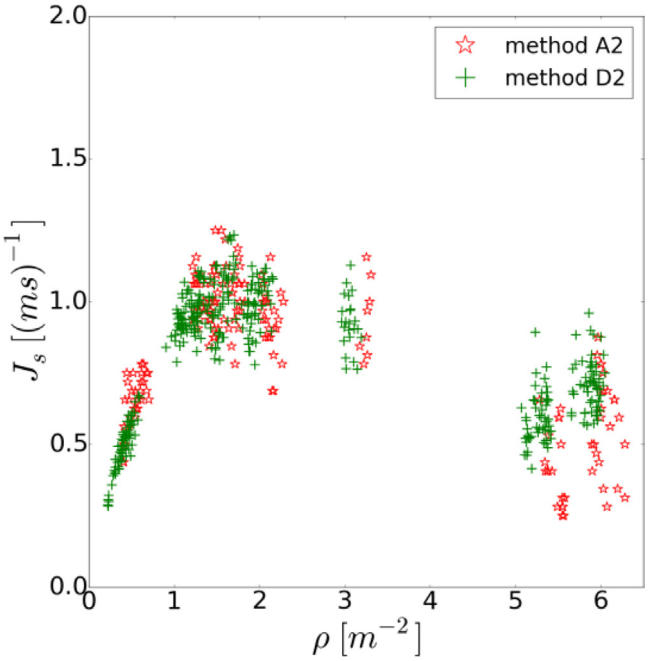

Figure 10. Comparison of fundamental diagrams of BaSiGo_Cross_A experiment with methods A2 and D2.

is used. By applying the procedure for all runs we obtain the fundamental diagrams shown in figure 7.

4.1. Comparison of measurement methods

Figures 8 and 9 show the fundamental diagrams of the four-directional cross flows experiment measured by different methods. The fundamental diagram can be divided into three regions: free flow region ($\rho \leqslant 1$ m^{-2}), capacity region (1 m$^{-2} < \rho < 4$ m^{-2}) and congested region ($\rho \geqslant 4$ m^{-2}). Figure 8 shows that the flow increases in the free flow region, is nearly constant in the capacity region and decreases in the congested region. Specifically, for the free flow region no difference is found for these three measurement methods. In the capacity region the specific flow at $\rho = 3$ m^{-2} is a little higher for method A1 than for methods A2 and A3. Also in the congested region the specific flow measured with method A1 is the largest but it is little higher measured with method A2 than with method A3. At the free flow regime no conflict occurs and pedestrians move with free velocity. With the increase of the density the frequency of conflicts increases and it becomes difficult to move forward. Under this circumstance some pedestrians prefer to detour just as P_1 in figure 4 or change the intended direction and go to another direction than originally intended just like P_2 in figure 4 in order to progress. These movements cause a higher flow if method A1 is used.

For the Voronoi methods D1 and D2 no difference appears in the fundamental diagrams in the free flow regime, see figure 9. With increasing density, velocity decreases leading to more pronounced body sway and detour behavior occurs as shown in figure 4, which causes deviations of the movement from the intended direction. Therefore, the

J. Stat. Mech. (2017) 033404

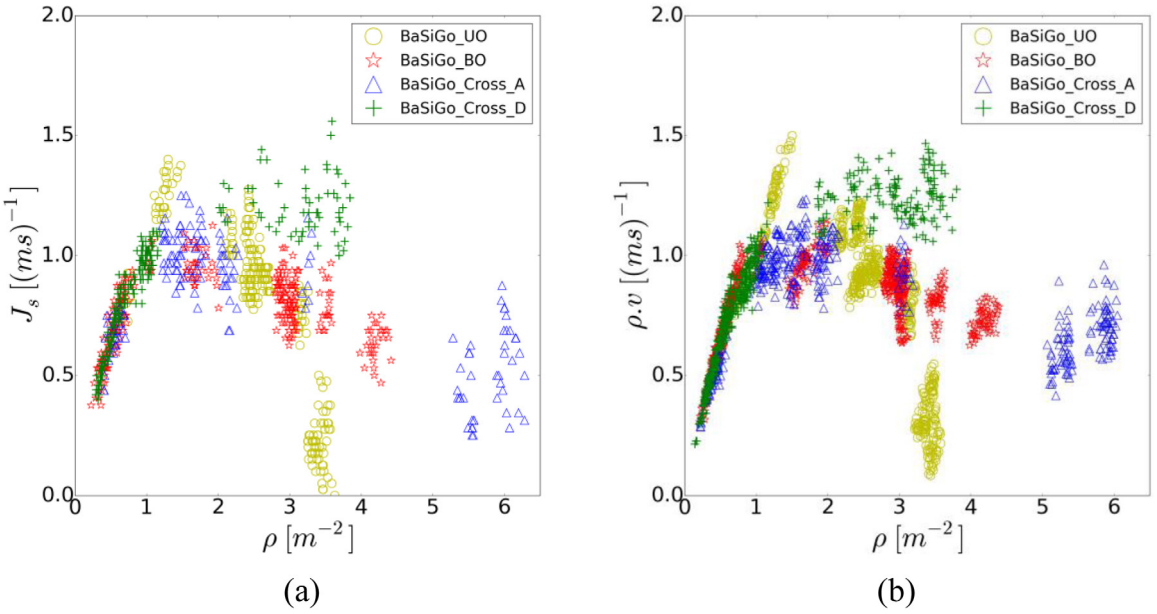

Figure 11. Comparison of fundamental diagrams of different flows with (a) method A2 and (b) method D2.

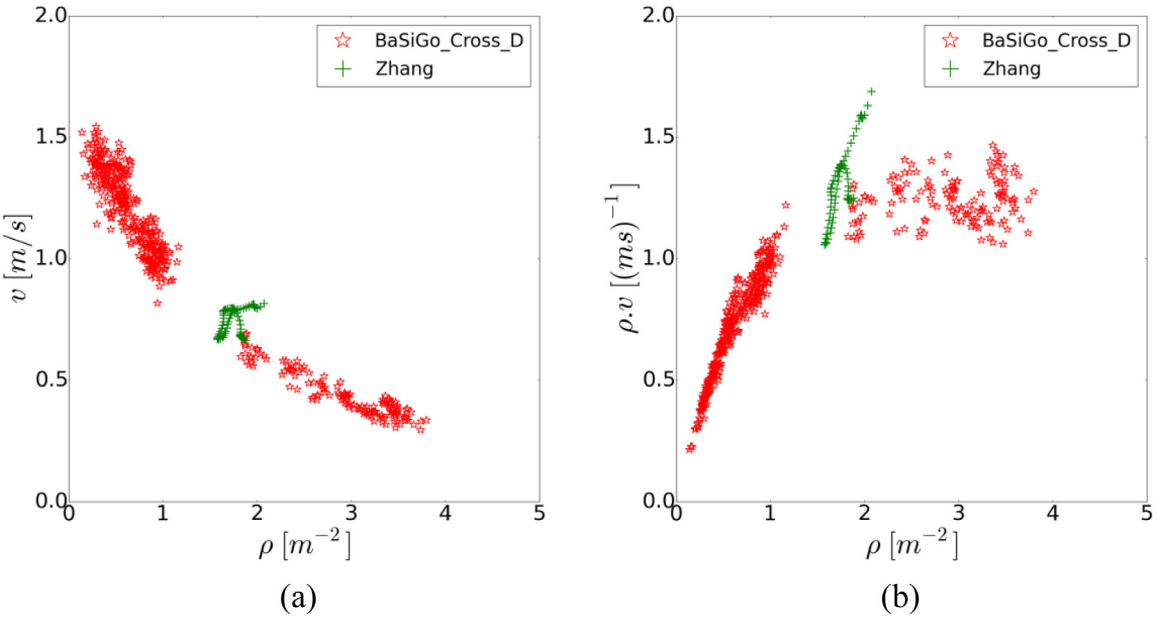

Figure 12. Comparison of fundamental diagrams of BaSiGo_Cross_D experiment with method D2 and Zhang's experiment [14]. (a) Density–velocity relation, (b) density–flow relation.

specific flow measured with method D2 considering the effective movement in the intended direction is smaller than with the classic method D1.

Figure 10 shows the comparison of method A2 and method D2. Significant differences can only be found at high densities. The specific flow with method A2 is smaller than with method D2 for $\rho > 5$ m^{-2}. Method A2 leads to the lower flow because it neglects

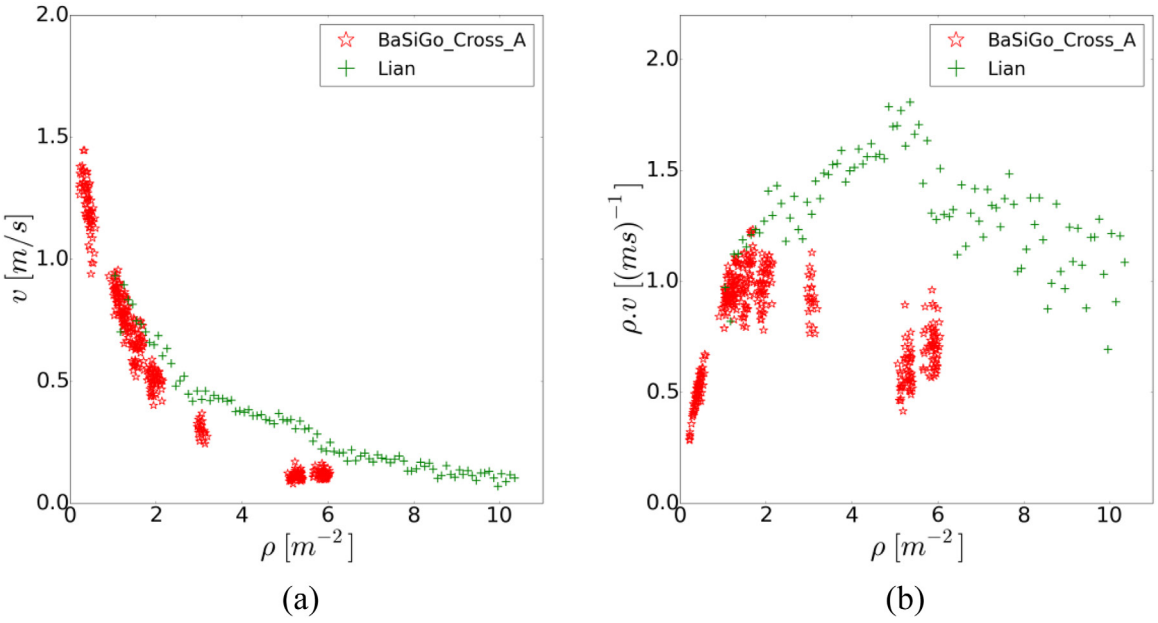

Figure 13. Comparison of fundamental diagrams of BaSiGo_Cross_A experiment with method D2 and Lian's experiment [16]. (a) Density–velocity relation, (b) density–flow relation.

movements in the cross area, while method D2 considers the contribution of pedestrians' velocity to the flow in the intended direction inside the cross area.

The results discussed above show that large differences exist in the fundamental diagrams if different measurement methods are used, especially for high density situations. The flow calculated with method A1 does not represent the flow as a measure for performance because it considers movements deviating from the intended direction, while these ineffective movements are neglected in methods A2 and A3. Similarly, method D2 calculates the flow which reflects the real contribution of pedestrian movement with respect to the intended direction when compared to method D1. As a result, it is more suitable to select method A2 (the difference between methods A2 and A3 is small and we just choose method A2) and method D2 for a comparison of fundamental diagrams of crossing streams, uni- and bidirectional streams.

4.2. Comparison of different pedestrian flows

In this section, unidirectional flow (BaSiGo_UO), bidirectional counter flow (BaSiGo_BO), bidirectional cross flow (BaSiGo_Cross_D) and four-directional cross flow (BaSiGo_Cross_A) are compared. Figure 11 shows the fundamental diagrams with method A2 and method D2. For densities $\rho < 1\ \mathrm{m}^{-2}$ there is no difference in the fundamental diagrams of these flows. Differences appear for the highest value of the specific flow $C_\mathrm{s} = J_\mathrm{s,max}$ at the critical density ρ_c where C_s appears. In order to guarantee the independence of the final results from the initial condition of the experiment. As a consequence, no data is obtained in some density intervals and the maximum specific flow is not reliable and determinable. A rough manual identification of the values for the specific flow around $\rho = 1.5\ \mathrm{m}^{-2}$ gives 1.4 $(\mathrm{m}\cdot\mathrm{s})^{-1}$, 1.1 $(\mathrm{m}\cdot\mathrm{s})^{-1}$, 1.2 $(\mathrm{m}\cdot\mathrm{s})^{-1}$ and 1.1 $(\mathrm{m}\cdot\mathrm{s})^{-1}$ for unidirectional flow, bidirectional counter flow, bidirectional cross flow

and four-directional cross flow respectively in figure 11. Consistent with our results, it has been shown in [3] that the maximum of the specific flow of unidirectional streams is significantly larger than of bidirectional counter flows.

For unidirectional flow and bidirectional counter flow, the specific flow decreases for $\rho > 1.5$ m^{-2}, however it keeps almost constant or slightly increases for bidirectional cross flow, which is different from the previous study [14] where Zhang *et al* analyzed experimental data from [27]. In addition, the maximum specific flow of bidirectional cross streams is also inbetween the values of unidirectional flow and bidirectional counter flow. These differences could be explained by the mixture of flow types occurring in the measurement area of BaSiGo_Cross_D experiment, see figures 1(c) and 2(c). In the cross area a mixture of unidirectional and bidirectional cross flows occur. At the entrance to the measurement area conflicts occur due to different moving directions. At the exit unidirectional movement dominates. Nevertheless, the data are limited and they only focus on the density interval around 2 m^{-2} in the experiment analyzed by Zhang [14] as shown in figure 12. The specific flow in [14] is higher than in the BaSiGo_Cross_D experiment around 2 m^{-2}. Factors which may contribute to the difference are: (1) experimental subjects. The participants in the BaSiGo experiments are composed of university students with the mean age of 25 years old, whereas in [14] they are volunteers from the event visitors and cover a wide range of age even including children; (2) experimental setup. The scenario in the BaSiGo experiments is set up by wooden boxes which are high enough to ensure pedestrians cannot see people from the other direction before they meet in the cross area, while no visual restriction exist in [14]. Thus the participants have the chance to anticipate possible conflicts with other pedestrians and avoid them; (3) measurement method. Method D1 containing the contribution of ineffective movement to the flow is adopted in [14], whereas method D2 considering the flow in the intended direction is used in our analysis.

It is interesting that the fundamental diagrams of four-directional cross streams are similar with those of the bidirectional counter flows. The maximum specific flow is also the same in these two flow types. However, the results differ from Lian's study [16] as displayed in figure 13. In [16] the specific flow increases continuously till $\rho = 5$ m^{-2} and reaches a highest value of 1.8 (m $\cdot$ s)$^{-1}$ which is significantly larger than 1.1 (m $\cdot$ s)$^{-1}$ measured in our study. Moreover, the maximum density exceeds $\rho = 10$ m^{-2} in [16] while it is about $\rho = 6.5$ m^{-2} in the experiment discussed in this study. Reasons responsible for these differences could be: (1) the motivations of experimental subjects in these two experiments are different. From the video of Lian's experiment we find pedestrians who are all males with an average age of 20 years are excited to rush to each other at the beginning of the experiment, which leads to a high velocity in the cross area. In our experiment the test persons are advised to walk normally and no rushing is observed; (2) the mean body size of Asian is smaller than of European, therefore the density in the experiment with Chinese test person could be higher and at the same density pedestrians have more space to move; (3) the measurement method based on a Gaussian distance dependent weight function is used in Lian's analysis [16] and the backward movements are considered as the negative contribution to the flow. In our analysis pedestrian flow is calculated using Voronoi diagrams and the effect of moving back is filtered out. All factors discussed above could be responsible for the differences of the result.

J. Stat. Mech. (2017) 033404

5. Conclusion

In our paper different measurement methods are proposed to calculate pedestrian flow for multidirectional streams. For low densities no difference is found in the fundamental diagrams using different measurement methods. However, the difference becomes obvious with increasing density. To get an enhanced description of the performance by measuring the flow we use methods A2 and D2. Method A2 filters the effect of detour on pedestrian flow and method D2 considers the intended direction. The shape of the fundamental diagrams of unidirectional, bidirectional counter, bidirectional cross and four-directional cross flows are analyzed and compared.

The bidirectional cross flow is spatial inhomogeneous and consists of a mixture of unidirectional flow and bidirectional counter flow. It is interesting that no difference is found in the fundamental diagrams between bidirectional counter flow and four-directional cross flow in the density range covered in these experiments. The comparisons with data from previous studies revealed large differences which could be caused by factors such as different measurement methods, different motivations of test subjects and different experimental setups. Our results contribute to empirical data of pedestrian dynamics and describe transport properties of the most usual but also most complex traffic system.

Acknowledgments

The foundation supports from the China Scholarship Council (CSC) and Key Research and Development Program of China (2016YFC0802508). The project BaSiGo has been supported by the German Federal Ministry for Education and Research. We thank Dr Liping Lian for offering the data of four directional cross flows experiment in their study.

References

[1] Zhang J, Klingsch W, Schadschneider A and Seyfried A 2011 Transitions in pedestrian fundamental diagrams of straight corridors and T-junctions *J. Stat. Mech.* P06004
[2] Kretz T, Grünebohm A, Kaufman M, Mazur F and Schreckenberg M 2006 Experimental study of pedestrian counterflow in a corridor *J. Stat. Mech.* P10001
[3] Zhang J, Klingsch W, Schadschneider A and Seyfried A 2012 Ordering in bidirectional pedestrian flows and its influence on the fundamental diagram *J. Stat. Mech.* P02002
[4] Hoogendoorn S and Daamen W 2004 Self-organization in walker experiments *Traffic and Granular Flow* vol 3 (Berlin: Springer) pp 121–32
[5] Flötteröd G and Lämmel G 2015 Bidirectional pedestrian fundamental diagram *Transp. Res.* B **71** 194–212
[6] Nikolic M, Bierlaire M, Farooq B and de Lapparent M 2016 Probabilistic speed–density relationship for pedestrian traffic *Transp. Res.* B **89** 58–81
[7] Garcimartín A, Parisi D, Pastor J, Martín-Gómez C and Zuriguel I 2016 Flow of pedestrians through narrow doors with different competitiveness *J. Stat. Mech.* 043402
[8] Liao W, Tordeux A, Seyfried A, Chraibi M, Drzycimski K, Zheng X and Zhao Y 2016 Measuring the steady state of pedestrian flow in bottleneck experiments *Physica* A **461** 248–61
[9] Ezaki T, Yanagisawa D and Nishinari K 2012 Pedestrian flow through multiple bottlenecks *Phys. Rev.* E **86** 026118
[10] Hoogendoorn S P and Daamen W 2005 Pedestrian behavior at bottlenecks *Transp. Sci.* **39** 147–59

J. Stat. Mech. (2017) 033404

[11] Seyfried A, Passon O, Steffen B, Boltes M, Rupprecht T and Klingsch W 2009 New insights into pedestrian flow through bottlenecks *Transp. Sci.* **43** 395–406
[12] Wong S, Leung W, Chan S, Lam W H, Yung N H, Liu C and Zhang P 2010 Bidirectional pedestrian stream model with oblique intersecting angle *J. Transp. Eng.* **136** 234–42
[13] Guo R Y, Wong S, Huang H J, Zhang P and Lam W H 2010 A microscopic pedestrian-simulation model and its application to intersecting flows *Physica* A **389** 515–26
[14] Zhang J and Seyfried A 2014 Comparison of intersecting pedestrian flows based on experiments *Physica* A **405** 316–25
[15] Bamberger J, Geßler A-L, Heitzelmann P, Korn S, Kahlmeyer R, Lu X H, Sang Q H, Wang Z J, Yuan G Z and Gauß M 2015 Crowd research at school: crossing flows *Traffic and Granular Flow'13* (Berlin: Springer) pp 137–44
[16] Lian L, Mai X, Song W, Richard Y K K, Wei X and Ma J 2015 An experimental study on four-directional intersecting pedestrian flows *J. Stat. Mech.* P08024
[17] Seyfried A, Boltes M, Kähler J, Klingsch W, Portz A, Rupprecht T, Schadschneider A Steffen B and Winkens A 2010 Enhanced empirical data for the fundamental diagram and the flow through bottlenecks *Pedestrian and Evacuation Dynamics 2008* ed W W F Klingsch *et al* (Berlin: Springer) pp 145–56
[18] Boltes M, Seyfried A, Steffen B and Schadschneider A 2010 Automatic extraction of pedestrian trajectories from video recordings *Pedestrian and Evacuation Dynamics 2008* (Berlin: Springer) pp 43–54
[19] Boltes M and Seyfried A 2013 Collecting pedestrian trajectories *Neurocomputing* **100** 127–33
[20] Mehner W, Boltes M, Mathias M and Leibe B 2015 Robust marker-based tracking for measuring crowd dynamics *Int. Conf. on Computer Vision Systems* (Berlin: Springer) pp 445–55
[21] Mehner W, Boltes M and Seyfried A 2016 Methodology for generating individualized trajectories from experiments *Traffic and Granular Flow'15* (Berlin: Springer) pp 3–10
[22] Kise K, Sato A and Iwata M 1998 Segmentation of page images using the area Voronoi diagram *Comput. Vis. Image Underst.* **70** 370–82
[23] Garrido S, Moreno L, Abderrahim M and Martin F 2006 Path planning for mobile robot navigation using voronoi diagram and fast marching *2006 IEEE/RSJ Int. Conf. on Intelligent Robots and Systems* (IEEE) pp 2376–81
[24] Boots B and South R 1998 Modeling retail trade areas using higher-order, multiplicatively weighted voronoi diagrams *J. Retail.* **73** 519–36
[25] Aziz N A B A, Mohemmed A W and Alias M Y 2009 A wireless sensor network coverage optimization algorithm based on particle swarm optimization and voronoi diagram *Int. Conf. on Networking, Sensing and Control, 2009. ICNSC'09* (IEEE) pp 602–7
[26] Steffen B and Seyfried A 2010 Methods for measuring pedestrian density, flow, speed and direction with minimal scatter *Physica* A **389** 1902–10
[27] Plaue M, Chen M, Bärwolff G and Schwandt H 2011 Trajectory extraction and density analysis of intersecting pedestrian flows from video recordings *Photogrammetric Image Analysis* (Berlin: Springer) pp 285–96

J. Stat. Mech. (2017) 033404